

## Effects of Sintering Time on Microstructure and Properties of Alumina Foam Ceramics

Z. Chu<sup>1, 2</sup>, C. Jia<sup>1, 2</sup>, J. Liu<sup>\*1, 2</sup>, R. Ding<sup>1, 2</sup>, G. Yuan<sup>3</sup>

<sup>1</sup>School of Material Science and Engineering, Shandong University of Technology, Zibo 255049, China

<sup>2</sup>National Engineering Research Center of Industrial Ceramics of China, 12 Zhangzhou Road, Zibo 255049, China

<sup>3</sup>Shandong Electric Shield Polytron Technologies Inc, Zibo 255000, China

received April 30, 2017; accepted July 2, 2017

### Abstract

As heat insulating materials, alumina foam ceramics possess many advantages such as low thermal conductivity, high thermostability, good wear resistance, high hardness, and excellent resistance to corrosion. In this paper, a high-alumina foam ceramic was prepared with the gel-foaming method using aluminum dihydrogen phosphate as gel, and alumina fibers as reinforcing component. The effects of sintering time on phase components, fiber surface morphology, microstructure, and mechanical properties of the samples were investigated. It was found that C-AIPO<sub>4</sub> with higher temperature stability demonstrated higher crystallinity, and increasing sintering time facilitated the conversion of T-AIPO<sub>4</sub> to C-AIPO<sub>4</sub>. Meanwhile, the porosity first decreased with time followed by an increase, and the compressive strength increased first and then decreased. When the sintering time is 4 h, the optimized compressive strength reached 4.3 MPa. So, the best sintering time is 4 h.

*Keywords:* Foam ceramics, alumina fibers, microstructure, compressive strength

### I. Introduction

As a porous material with high-temperature tolerance, foam ceramic was firstly prepared with alumina, kaolin, and other raw materials<sup>1</sup>. Foam ceramic has numerous merits, such as low density, high porosity, high temperature resistance, high specific strength, and high corrosion resistance. It is widely used in metal solution filtration, heat insulation and sound insulation materials, automobile exhaust treatment, electronic devices, medical equipment, and biochemistry. First, a wide range of methods was studied to prepare ceramic foams. Ren *et al.*<sup>2</sup> prepared a new type of SiC ceramic foam with epoxy resin matrix and SiC, and found that the manufacturing transition layer could improve the mechanical properties of the SiC foam ceramic effectively. Li *et al.*<sup>3</sup> prepared alumina foam ceramics with varying porosity by means of organic impregnation with a gel injection molding process. Porosity plays a vital role in the physical properties of foam ceramics. High porosity generally reduces the density and thermal conductivity of the ceramic. The relationship between the porosity and the material has been studied extensively. Yuan *et al.*<sup>4</sup> studied the effect of alumina powder size on the porosity and microstructure of the ceramic. The results showed that the porosity of the ceramics prepared from the nanoscale Al<sub>2</sub>O<sub>3</sub> powder was 1.3%. Sciamanna<sup>5</sup> prepared alumina foam ceramic by adding a suspension of butyric acid containing alumina, and ana-

lyzed the microstructure and mechanical properties of the alumina foam ceramics. The flexural strength of the ceramic was 502 MPa. However, the strength of the material also weakens with increasing porosity. To overcome this challenge, many approaches have been proposed to increase the porosity while maintaining the strength. Ceramic matrix composites reinforced by fibers have become the research focus owing to their high temperature tolerance, enhanced strength, good chemical stability, high elastic modulus, and good rigidity. Ma *et al.*<sup>6</sup> studied the mechanism of alumina-fiber-toughened alumina ceramic. The results showed that the bending strength of the material under high temperature was improved. Lang *et al.*<sup>7</sup> prepared porous YSZ by Al<sub>2</sub>O<sub>3</sub> fiber, and studied the effects of the sintering temperature, sintering time, and Al<sub>2</sub>O<sub>3</sub> fiber content on the porosity, microstructure, compressive strength, and fracture toughness of the sample. As the fiber content was 10 vol%, the compressive strength and flexural strength were 100.2 MPa and 61.5 MPa, respectively. Liu *et al.*<sup>8</sup> studied the effects of fiber dosage on the mechanical properties of the composite. The strength and fracture toughness of the material were better with 5% fiber content. Alumina foam ceramic reinforced by alumina fiber has attracted a lot of attention thanks to its excellent oxidation resistance under high temperature. At different sintering times, the ceramic matrix and fiber are affected differently, so the properties of the material are affected. Hou *et al.*<sup>9</sup> studied the effect of sintering time on the strength and open porosity of biological SiC ceramics.

\* Corresponding author: [jchliu@sdut.edu.cn](mailto:jchliu@sdut.edu.cn)

With an increasing sintering time, the porosity of the ceramic decreased, while the flexural strength and fracture toughness increased. Dai *et al.*<sup>10</sup> studied the effects of sintering time on intergranular phase and mechanical properties of silicon nitride ceramics. The results showed that the total grain content, boundary phase, density, and strength of the samples increased with the increase in sintering time. Sutharsini<sup>11</sup> studied the effects of sintering time on the microstructure and properties of porous  $\alpha$ -Si<sub>3</sub>N<sub>4</sub>/Sialon composite coatings. With the increase of sintering time, the hardness and fracture toughness of the Si<sub>3</sub>N<sub>4</sub> ceramics were notably improved.

Previous work demonstrates that the sintering time has a significant impact on the physical properties of the alumina matrix and alumina fibers. In this paper, a high-alumina foam ceramic was prepared with the gel-foaming method using water as dispersing medium, and aluminum dihydrogen phosphate as gel and alumina fiber as reinforcing component. The effects of sintering time on the phase composition, fiber surface morphology, microstructure, and mechanical properties of the samples were investigated.

## II. Experimental

### (1) Experimental materials

Alumina powder (99.99%,  $d_{50} = 0.5 \mu\text{m}$ ) was used as a precursor. H-WF-3 ultra-fine high-white aluminum hydroxide powder (also known as aluminum trihydrate powder,  $d_{50} = 3.16 \mu\text{m}$ , 64.9% alumina content, China Aluminum Co., Ltd.) and OP-10 (nonionic surfactant with nonylphenol polyoxyethylene ether as the main ingredient, HLB is 14.5, Laiyang Economic and Technological Development Zone Fine Chemical Co., Ltd.) were used as emulsifier. 97% polycrystalline alumina fiber (Zhejiang Deqing Jiahe Crystal Fiber Co., Ltd) was used as enhancement. At high temperatures, the polycrystalline alumina fiber always maintains polycrystalline microcrystalline structure, thus ensuring excellent heat resistance, high thermal stability, and high temperature stability. The surface of the polycrystalline alumina fiber is smooth and well-shaped with relatively high L/D. The fibers were cut into segments with length of 1–2 mm. Aluminum dihydrogen phosphate (99.99%, Pei You Biotechnology (Shanghai) Co., Ltd.) was used as the gelling agent.

### (2) Sample preparation

The ceramic samples were prepared with the gel-foaming method. The process included slurry preparation, mixing, molding, drying, and sintering. The mass ratio of alumina powder, aluminum hydroxide, alumina fiber, and aluminum dihydrogen phosphate was 0.51 : 0.08 : 0.10 : 0.31. The aluminum dihydrogen phosphate solution (60 wt%) was prepared with aluminum dihydrogen phosphate and deionized water. Next, alumina powder, aluminum hydroxide powder, and alumina fiber were sequentially added into aluminum dihydrogen phosphate solution to form a slurry. Deionized water was used to adjust the viscosity of the slurry. Subsequently, the mixture was stirred for 2–3 h until a constant slurry volume was reached. Afterwards, the slurry was cast into a disc-shaped

mold with a diameter of 13.5 cm. The mold was kept still for 24 h at room temperature until the slurry gelled. The green body was oven-dried at 50 °C for about 2 days, then sintered at 1580 °C for 2, 4, 6, and 8 h. The corresponding samples are labeled (a) 2 h, (b) 4 h, (c) 6 h, and (d) 8 h, respectively.

### (3) Characterization

The phase composition of the sintered samples was analyzed using a D8 Advanced X-ray diffractometer (XRD, Germany) with CuK $\alpha$ 1 radiation at an accelerated voltage of 40 kV and a scanning step of 0.02 degree. The microstructure was observed with a Sirion 200 scanning electron microscopy (SEM, Holland). The compressive strength was measured with an electronic universal testing machine. The open porosity of the samples was measured with the Archimedes method. The slurry viscosity was examined with a rotational viscometer.

## III. Results and Discussion

### (1) Effects of sintering time on the phase composition of samples

Fig. 1 shows the effects of sintering time on the phase composition of the samples. It can be seen that only the diffraction peaks of C-AlPO<sub>4</sub>,  $\alpha$ -Al<sub>2</sub>O<sub>3</sub>, and T-AlPO<sub>4</sub> phase are shown in the XRD curves in Fig. 1. This indicates that the sintering time has no effects on the phase composition of the samples. The peak intensity of C-AlPO<sub>4</sub> increases, indicating an improved crystallinity. The peak intensity of T-AlPO<sub>4</sub> decreases with the increase of the sintering time. The peak intensity of  $\alpha$ -Al<sub>2</sub>O<sub>3</sub> shows no apparent change with the increase of sintering time. At high temperature of 1580 °C, AlPO<sub>4</sub> mainly exists in the stable phase of C-AlPO<sub>4</sub> and  $\alpha$ -Al<sub>2</sub>O<sub>3</sub>. Sintering at high temperature can transform T-AlPO<sub>4</sub> into C-AlPO<sub>4</sub>. Therefore, with the increase of sintering time, the crystallinity of C-AlPO<sub>4</sub> becomes higher, and the corresponding T-AlPO<sub>4</sub> is converted to C-AlPO<sub>4</sub>. The relative content of T-AlPO<sub>4</sub> decreases and the crystallinity of  $\alpha$ -Al<sub>2</sub>O<sub>3</sub> does not change much.

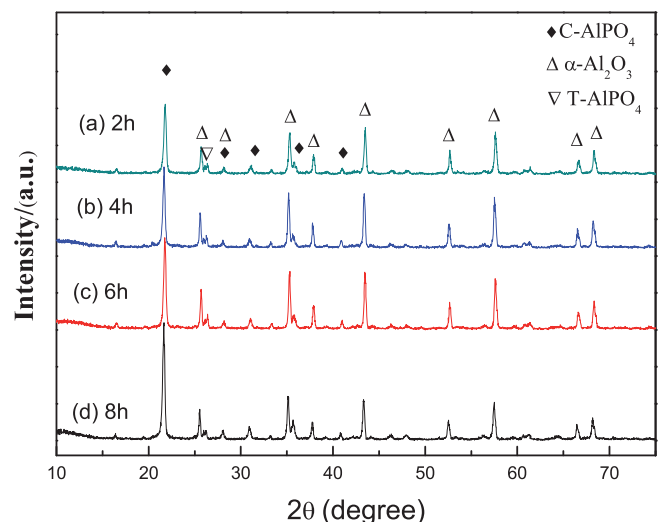


Fig. 1: XRD patterns of samples with various sintering times.

## (2) Effects of sintering time on the surface morphology of the fibers

Fig. 2 shows the effects of the sintering time on the surface morphology of the fibers. It can be seen that when the sintering time is 2 h, the alumina fibers are bonded loosely to the alumina matrix, with a gap between the fiber and the matrix (Fig. 2a). In Fig. 2b, when the sintering time is 4 h, the bond is enhanced between the fiber and the matrix. There is no void between the matrix and the fiber. Note the cross-section of the fiber is thicker owing to a non-uniform fiber diameter distribution in the sample. As shown in Fig. 2c, when the sintering temperature reaches 6 h, the particle size on the fiber surface increases significantly so that the surface of the fiber becomes rough, resulting in a gap between the fiber and the alumina particles. In Fig. 2d, as the sintering time further increases to 8 h, the particle growth on the alumina fiber surface continues to increase, covering the entire surface of the fiber. As a result, the flexibility of the fibers is reduced, as the grain accumulation on the fiber surface reduces the role of the alumina fibers in the ceramic matrix.

In the zoom-in SEM images, as shown in Fig. 3, more details are revealed on the sintering effect. It can be seen that

when the sintering time is 2 h, the grain of the fiber is small and the surface is rough (Fig. 3a). In Fig. 3b, when the sintering time is 4 h, the grain of the fiber becomes larger and more uniform, and the surface is smoother and the degree of densification is deepened. With the extension of sintering time, the grains of the fiber begin to grow slowly. In Fig. 3c, when the sintering time is 6 h, the size of the grain increases, and the uniformity of the grain becomes poorer. In Fig. 3d, when the sintering time reaches 8 h, it is clear that the fiber cross-section becomes rugged, and the surface of the fiber is occupied by large grains with irregular shape and coarse grain boundaries. These phenomena are typical for over-burning of fibers. As the sintering time is prolonged, the larger crystal grains have lower surface energy than the smaller grains, so the larger grains continue to grow under the surface driving force. The results show that the sintering time indeed has a great influence on the surface morphology of the fiber at the same sintering temperature. With the increase of the sintering time, the fiber cross-section becomes uneven owing to uneven grain growth. At the same time, the grain growth on the fiber surface becomes more significant, introducing more pores.

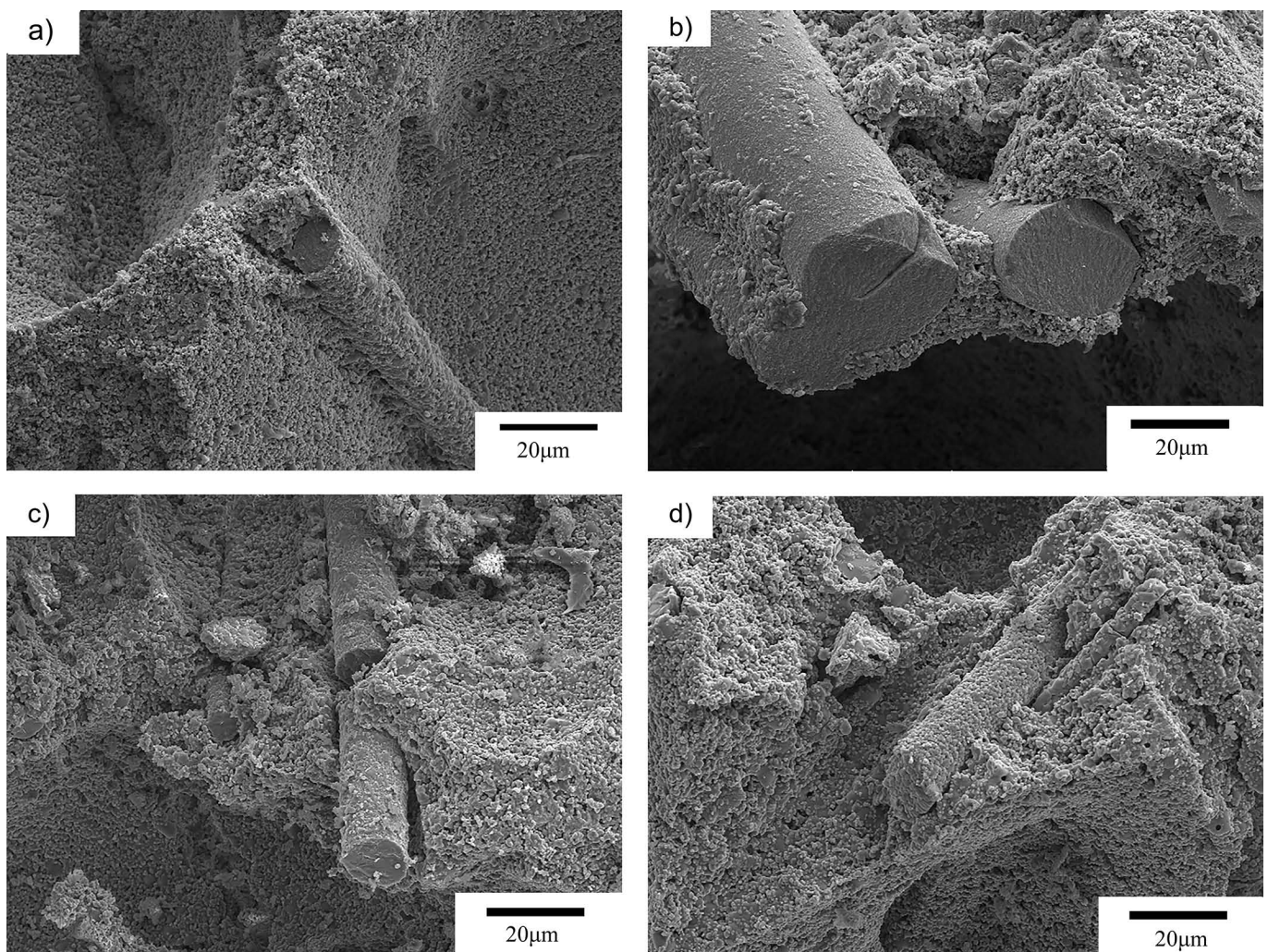


Fig. 2: Tilted view of SEM images of samples with various sintering times (Fig. 2a: 2 h sintering time, Fig. 2b: 4 h sintering time, Fig. 2c: 6 h sintering time, Fig. 2d: 8 h sintering time).

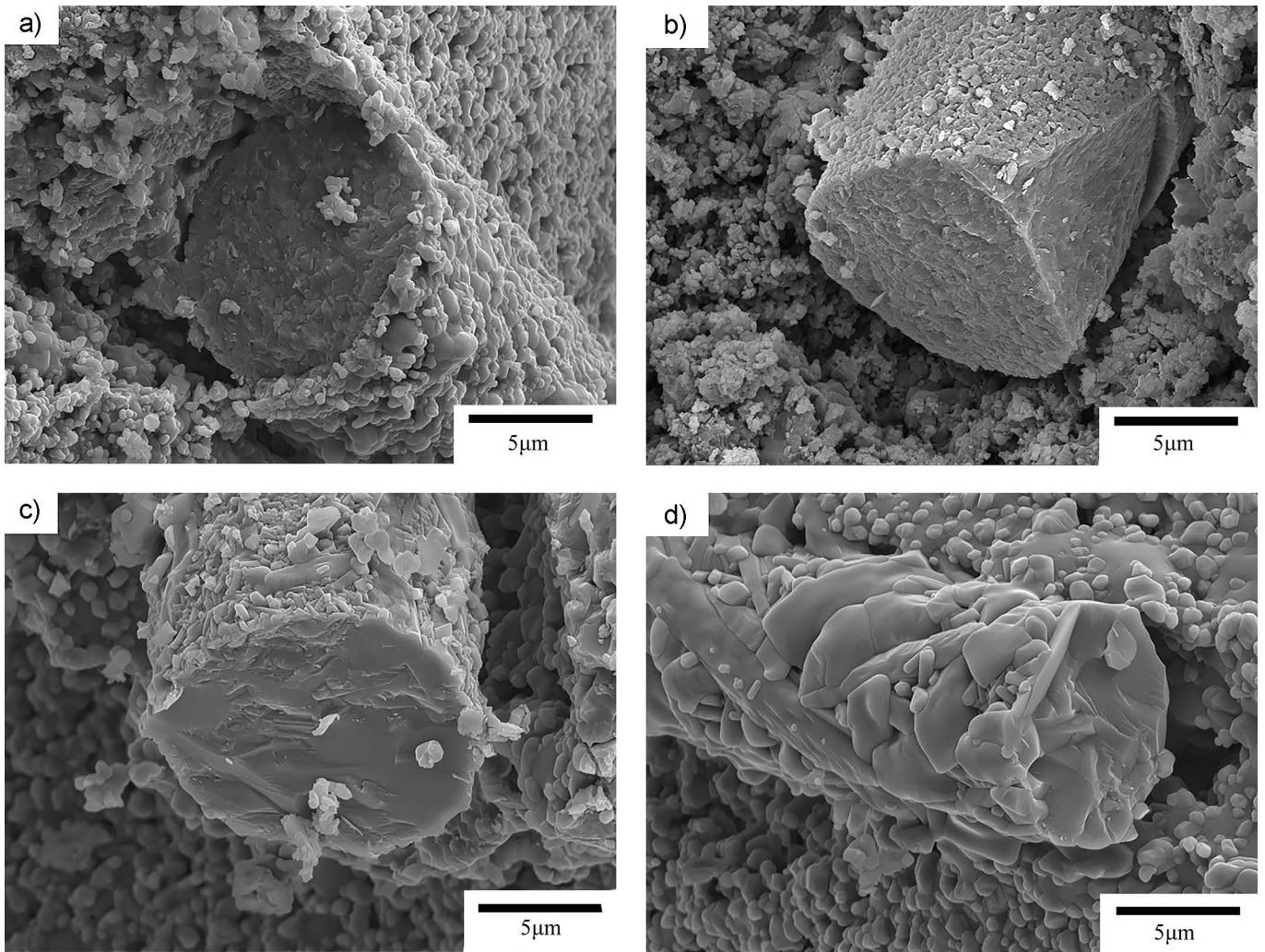


Fig. 3: Zoom-in SEM images of samples with various sintering times (Fig. 3a: 2 h sintering time, Fig. 3b: 4 h sintering time, Fig. 3c: 6 h sintering time, Fig. 3d: 8 h sintering time).

### (3) Effects of sintering time on the microstructure of the samples

Fig. 4 shows the effects of sintering time on the microstructure of the samples. In Fig. 4a, when the sintering time is 2 h, the grains are relatively small, and the grain sizes are non-uniform. A large number of voids are observed in the sample. In Fig. 4b, when the sintering time is 4 h, the grains grow obviously larger with more uniform size distribution. The internal voids of the sample are significantly smaller than those in the sample in Fig. 4a. In Fig. 4c, when the sintering time is 6 h, large grains begin to appear, and the intergranular grains are accumulated. The internal voids of the specimens increase. In Fig. 4d, when the sintering time reaches 8 h, the average size of the grains is larger with non-uniform distribution. The porosity of the sample is obviously increased compared to Fig. 4c. This shows that as the sintering time continues to increase, ceramic particles continue to grow. The size of the three-dimensional pore in the sample also increases.

According to the grain growth dynamics, the driving force can be expressed as:

$$F = \frac{2\delta}{R} \quad (1)$$

where  $F$  is the driving force,  $\delta$  is the specific surface energy, and  $R$  is the grain size in the formula. It can be seen that if specific interfacial energy is greater, the size of grains is smaller, and grain growth driving force  $F$  will be greater. The crystal face of the large crystal grains has a lower specific surface energy compared to the adjacent small grains. Therefore, with increased sintering time, the interface of the large grains is driven by the interfacial energy to move toward the center of the grain with small radius of curvature. The ceramic particles grow and the small grains gradually decrease or even disappear.

According to the grain growth thermodynamic driving force formula:

$$D^n - D_0^n = A \exp\left(-\frac{Q}{RT}\right) t \quad (2)$$

where  $D_0$  and  $D$  denote the initial grain size and the grain size at isothermal sintering time,  $n$  is the grain growth index,  $A$  is the grain growth rate constant,  $Q$  is the isothermal grain growth activation energy, and  $R$  is gas constant. It can be seen that the size of the grains increases with sintering time, which is in accordance with the experimental results. Owing to the higher surface free energy of the smaller grains, the smaller gains tend to grow larger to reduce the free energy. The material is suitably insulated in the sintering process, which can make the raw material reaction

more complete, promote grain boundary migration, and cause the grain to grow unceasingly. Nevertheless, longer sintering time will lead to abnormal grain growth. The degree of material densification decreases, resulting in deformation of the green body.

**(4) Effects of sintering time on the properties of alumina foam**

Fig. 5 demonstrates the effects of the sintering time on the porosity of the samples. As can be seen from Fig. 5, when the sintering temperature is 1580 °C, the porosity of the sample decreases first, and then increases with the sintering time. As the sintering time reaches 4 h, the free energy of the sample decreases with a decreasing solid/gas boundary area and an increasing solid/solid boundary area. The particles migrate and attach to each other, filling the pores inside the material and leading to reduced porosity of the material. As the sintering time further increases, the over-long sintering time results in significant growth of large ceramic grains. The grains form a 3D network structure with large numbers of voids inside the material. Thus, the porosity of the material increases again.

Fig. 6 shows the effects of sintering time on the compressive strength of the samples. As can be seen from Fig. 6,

when the sintering temperature is 1580 °C, the compressive strength of the samples increases first, and then decreases with the sintering time. On one hand, the strength of alumina ceramic foam decreases with increasing porosity. On the other hand, the fiber can enhance the structure of alumina foam ceramic, and thus enhance the strength of the ceramic foam. Overall, the compressive strength of alumina ceramic foam is greatly affected by porosity and fiber. As can be seen from Fig. 2, Fig. 3, and Fig. 4, when the sintering time is 2 h, the alumina fibers are loosely bonded to the alumina particles, and there is a gap between the fibers and the particles. The ceramic particles are not completely fused with high porosity, which results in a smaller compressive strength. When the sintering time is 4 h, the bond between the fiber and the particles is stronger, and the grain grows to a certain extent. The effect of fiber reinforcement is fully reflected, and the compactness of the sample is good with low porosity. The measured compressive strength is 4.3 MPa. As the sintering time increases, the molten alumina particles accumulate on the surface of the alumina fibers, and cause the grains to grow unevenly. As a result, the surface of the fibers becomes rough, which makes it difficult for the fibers to be pulled out and affects the reinforcing effect of the fibers.

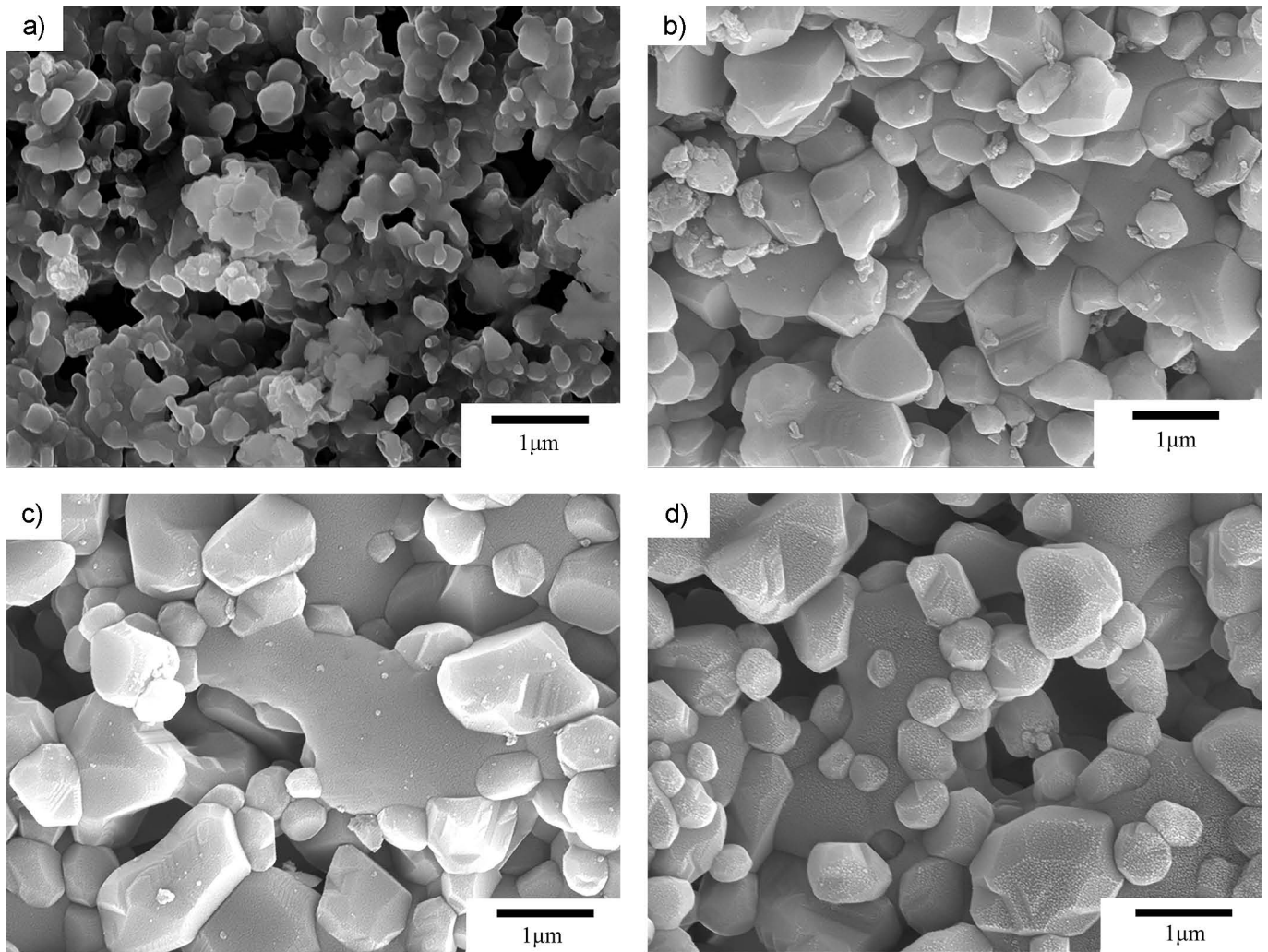


**Fig. 4:** Top view SEM images of samples with various sintering times (Fig. 4a: 2 h sintering time, Fig. 4b: 4 h sintering time, Fig. 4c: 6 h sintering time, Fig. 4d: 8 h sintering time).

Because the grains grow irregularly, the ability of the fiber to bear external force is reduced when external load is applied. The compressive strength of the sample is reduced owing to the increase in porosity, which is caused by the mutual stack among the grains.

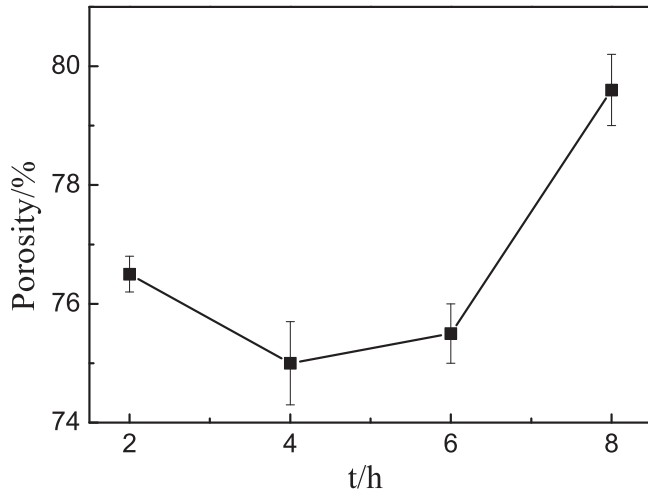


Fig. 5: Effects of the sintering time on the porosity of the samples.

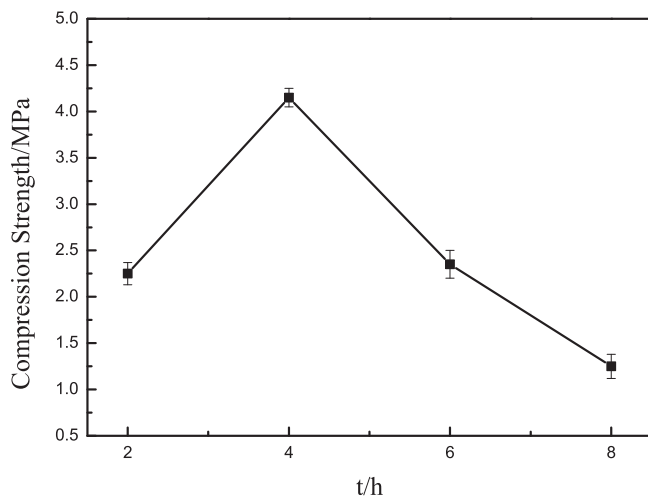


Fig. 6: Effects of the sintering time on the compressive strength of the samples.

#### IV. Conclusions

A high-alumina foam ceramic was prepared with the gel-foaming method using water as dispersing medium, aluminum dihydrogen phosphate as gel, and alumina fiber as reinforcing component. The effects of sintering time on the phase composition, fiber surface morphology, microstructure, and mechanical properties of the samples were studied. The following conclusions were obtained:

(1) For C- $\text{AlPO}_4$ , increased sintering time results in improved crystallinity. The corresponding T- $\text{AlPO}_4$  is con-

tinuously converted into C- $\text{AlPO}_4$ , but the  $\alpha$ - $\text{Al}_2\text{O}_3$  crystallinity is less affected.

(2) As the sintering time is increased, the cross-section of the fiber becomes irregular owing to uneven grain growth. The grains grow and form pores, which reduces the ability of the fiber to bear external force under applied load. With the increase in sintering time, the ceramic particles continue to grow and the sizes of the three-dimensional pores increase.

(3) With the increase of sintering time, the porosity of the sample decreases first and then increases, and the compressive strength increases first and then decreases. When the sintering time is 4 h, the compressive strength reaches 4.3 MPa. So the best sintering time is 4 h.

#### Acknowledgements

This work was financially supported by Shandong province science and technology major special project, Grant No. 2015ZDXX0402C05, and by University-City Cooperation Project of Zibo, Grant No. 2016ZBXC172.

#### References

- Zhu, X.W., Jiang, D.L., Tan, S.H., Zhang Z.Q.: Improvement in the thickness of reticulated porous ceramics, *J. Am. Ceram. Soc.*, **84**, 1654–1656, (2001).
- Ren, Z.H., Jin, P., Cao, X.M., Zhang, J.S.: Mechanical properties and slurry erosion resistance of SiC ceramic foam/epoxy co-continuous phase composite, *Compos. Sci. Technol.*, **107**, 129–136, (2015).
- Li, F.Z.: Study on the preparation technology of alumina porous ceramics with controllable porosity, (in Chinese), *Ceram.*, **2**, 24–27, (2009).
- Yuan, L., He, Z.B., Yu, J.K.: Preparation of closed porous alumina-based ceramics by superplastic high-temperature foaming, (in Chinese), *J. Northeast Univ.*, **34**, 939–943, (2013).
- Sciamanna, V., Nait-Ali, B., Gonon, M.: Mechanical properties and thermal conductivity of porous alumina ceramics obtained from particle stabilized foams, *Ceram. Int.*, **41**, 2599–2606, (2015).
- Ma, L.J., Jiang, M.X.: Study on the mechanism of toughened alumina ceramics by alumina fibers, (in Chinese), *Refract.*, **41**, 149–150, (2007).
- Lang, Y., Wang, C.A.:  $\text{Al}_2\text{O}_3$ -fiber-reinforced porous YSZ ceramics with high mechanical strength, *Ceram. Int.*, **40**, 10329–10335, (2014).
- Liu, N., Ye, R.L.: Inorganic fiber reinforced ceramic composite, *B. Chin. Ceram. Soc.*, **04**, 64–70, (1989).
- Hou, G.Y., Jin, Z.H., Qian, J.M.: Effect of holding time on the basic properties of biomorphic SiC ceramic derived from beech wood, *Mater. Sci. Eng.*, **452–453**, 278–283, (2007).
- Dai, J.Q., Huang, Y., Xie, Z.P., Ma, T., Yang, J.L., Ma, J.T.: Effects of holding time on intergranular phase and mechanical property of GPS silicon nitride ceramics, *J. Inorg. Mater.*, **18**, 91–97, (2003).
- Sutharsini, U., Ramesh, S., Wong, Y.H.: Effect of sintering holding time on low-temperature degradation of yttria stabilised zirconia ceramics, *Mater. Res. Innov.*, **18**, 408–411, (2014).